# Electronic Supplementary Information

## Self-assembly of Photoresponsive Azo-containing Phospholipids with a Polar Group as the Tail

Su Ma[a,b], Seiji Kurihara[a*], Yasuhiro Tomimori[a], Sunnam Kim[a], Eunsang Kwon[c], Atsushi Muramatsu[d], and Kiyoshi Kanie[d*]

[a]Department of Applied Chemistry and Biochemistry, Graduate School of Science and Technology, Kumamoto University, 2-39-1 Kurokami, Chuo-ku, Kumamoto, 860-8555, Japan.
E-mail: kurihara@gpo.kumamoto-u.ac.jp

[b]School of Chemistry, Biology and Material Engineering, Suzhou University of Science and Technology, No. 99 Xuefu Road, Huqiu district, Suzhou, 215009, China

[c]Graduate School of Science Research and Analytical Center for Giant Molecules, Tohoku University, 6-3 Aramakiazaaoba, Aoba-ku, Sendai, 990-8578, Japan

[d]Institute of Multidisciplinary Research for Advanced Materials, Tohoku University, Katahira 2-1-1, Aoba-ku, Sendai 980-8577, Japan
E-mail: kanie@tohoku.ac.jp

# Table of contents

## 1. Characterization of N6, M6, and N3

NMR spectra were measured in $CD_3OD$ solutions. $^1H$ NMR spectra were recorded on a JEOL JNM-LA400 at 400 MHz. The chemical shifts of the $^1H$ NMR signals were referenced to $Me_4Si$ as the internal standard ($\delta = 0.00$) and are expressed as chemical shifts in ppm ($\delta$), multiplicity, coupling constant (Hz), and relative intensity. Elemental analyses were carried out by the Elemental Analysis Laboratory, Institute of Multidisciplinary Research for Advanced Materials, Tohoku University, using a Yanako MT-6 CHN Corder. The compounds N6, M6 and N3 were determined as follows:

**N6**: M.p. = 253.8-254.9 °C. 1H-NMR (400 MHz, CD3OD), δ (TMS, ppm): 8.39 (d, J = 9 Hz, 2H), 8.02 (d, J = 9 Hz, 2H), 7.96 (d, J = 9 Hz, 2H), 7.09 (d, J= 9 Hz, 2H), 4.28-4.23 (m, 2H), 4.11 (t, J = 6 Hz, 2H), 3.94 (tt, J = 6, 6 Hz, 2H), 3.62-3.60 (m, 2H), 3.21 (s, 9H), 1.87-1.81 (m, 2H), 1.73-1.66 (m, 2H), 1.54-1.48 (m, 4H). Elemental analysis: Calculated for C23H33N4O7P (+2H2O) (%): C, 50.73; H, 6.85; N, 10.29. Found (%): C, 50.74; H, 6.62; N, 10.27.

**M6**: M.p. = 239.7-241.9 °C. 1H-NMR(400 MHz, CD3OD), δ (TMS, ppm): 7.85 (d, J = 3 Hz, 2H), 7.83 (d, J = 3 Hz, 2H), 7.05 (d, J =3 Hz, 2H), 7.02 (d, J =3 Hz, 2H), 4.26-4.22 (m, 2H), 4.07 (t, J = 6 Hz, 2H), 3.93 (tt, J = 6, 6 Hz, 2H), 3.78 (s, 3H), 3.62-3.59 (m, 2H), 3.21 (s, 9H), 1.85-1.81 (m, 2H), 1.71-1.67 (m, 2H), 1.55-1.50 (m, 4H). Elemental analysis: Calculated for C24H36N3O6P (+2H2O) (%): C, 54.46; H, 7.62; N, 7.94. Found (+2H2O) (%): C, 54.44; H, 7.56; N, 7.93.

**N3**: M.p. = 243.1-244.8 °C. 1H-NMR (400 MHz, CD3OD), δ (TMS, ppm): 8.39 (d, J = 9 Hz, 2H), 8.02 (d, J = 9 Hz, 2H), 7.98 (d, J = 9 Hz, 2H), 7.13 (d, J= 9 Hz, 2H), 4.28-4.23 (m, 4H), 4.12-4.08 (m, 2H), 3.59 (t, J = 4 Hz, 2H), 3.19 (s, 9H), 2.17-2.14 (m, 2H). Elemental analysis: Calculated for C20H27N4O7P (+1.5H2O) (%): C, 48.68; H, 6.13; N, 11.35. Found (%): C, 48.63; H, 6.16; N, 11.25.

## 2. Crystal data and X-ray single crystal structure of N3

For the evaluation of the self-assembling structure of **N6** and **N6**/**M6** mixtures, x-ray single crystal structure analysis of **N3** was carried out. The single crystal was obtained by slow cooling of aqueous hot solution of **N3** containing acetonitrile. The crystal data were collected by a R-AXIS RAPID diffractometer using multi-layer mirror monochromated Cu-Kα radiation at 90 K, and the crystal structure was analyzed using the SHELXL within the OLEX-2 GUI for modelling the molecular structures. The refined data for **N3** are as follows: Triclinic, space group *P*-1 (No. 2), $(C_{20}H_{27}N_4O_7P)\cdot 3H_2O$; $a$ = 8.3108(3), $b$ = 11.6756(3), $c$ = 25.7039(8) Å, $\alpha$ = 81.273(6) °, $\beta$ = 88.301(6) °, $\gamma$ = 83.153(6) °; $V$ = 2447.51(14) Å$^3$; $Z$ = 4; R = 0.1060, $w$R$_2$ = 0.2386.

Crystallographic data of **N3** has been deposited with Cambridge Crystallographic Data Center, deposition no. CCDC 2003927.

Figure S1 shows a molecular structure (ORTEP) and the single crystal structure of **N3** viewed along *a*-, *b*-, and *c*-axes.

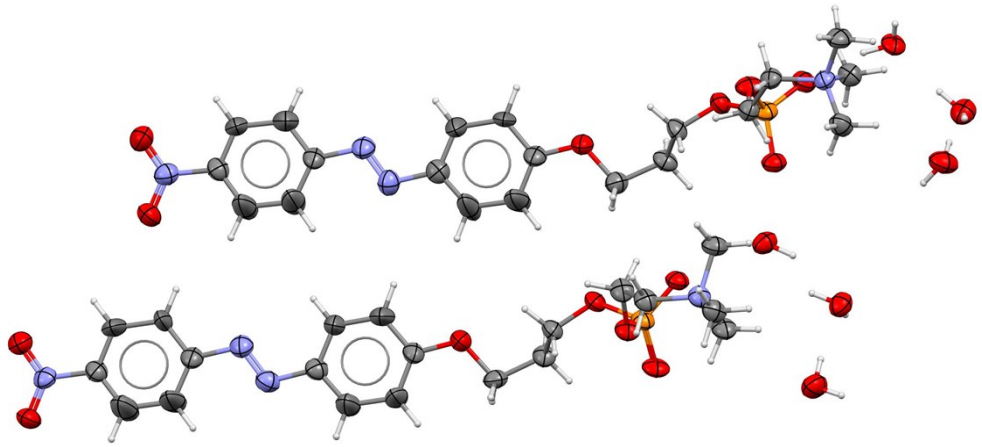

ORTEP of **N3**

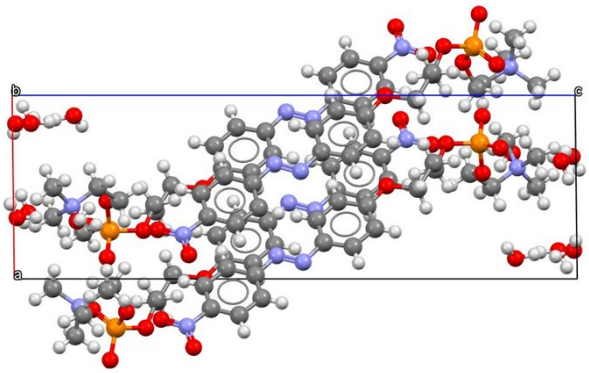

along b axis

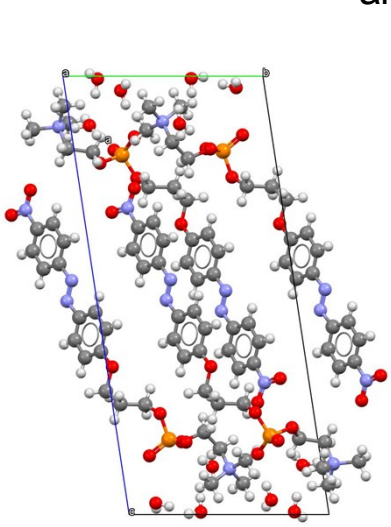

along a axis

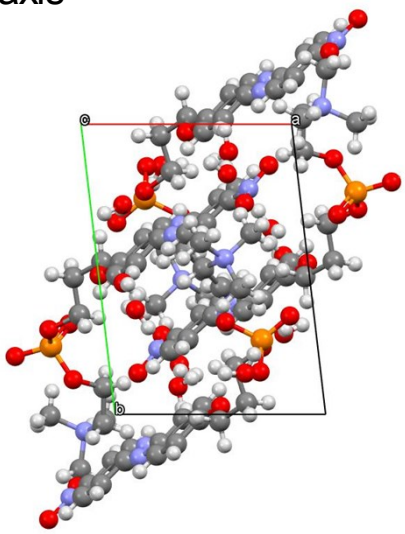

along c axis

**Figure S1.** ORTEP diagram (thermal ellipsoids drawn at 50% probability) and An X-ray single crystal structure of **N3**.

Figure S2 (a), (b), and(c) shows the single crystal structure of **N3**, high lightened water positions in the crystal, viewed along *b*-, *a*-, and *c*-axes, respectively. Compound **N3** forms tilted bilayer structure through *H*-aggregation of the **Az** moieties. Yellow-colored spheres in the Figures represent water molecules in the crystal. The water molecules were occupied interlayer between the bilayers of the **N3** molecules. Figure 2(d) shows the part of the crystal structure of **N3** focusing on the phosphocholine-moiety to clarify the formation mechanism of the stacked bilayer of **N6**. The magenta-colored part represents the phosphocholine-moiety of N3. The part bended away from the long axis of the **Az** skeleton to increase the affinity for the water layer through hydrogen bonding. The bending behavior of the phosphocholine moiety might enable phospholipids without a long alkyl tail to form a bilayer-type self-assembled structure through *H*-aggregation. Actually, it is impossible for the hydrophilic parts amphiphiles with only ammonium moieties but no phosphocholine moiety to bend in this way.

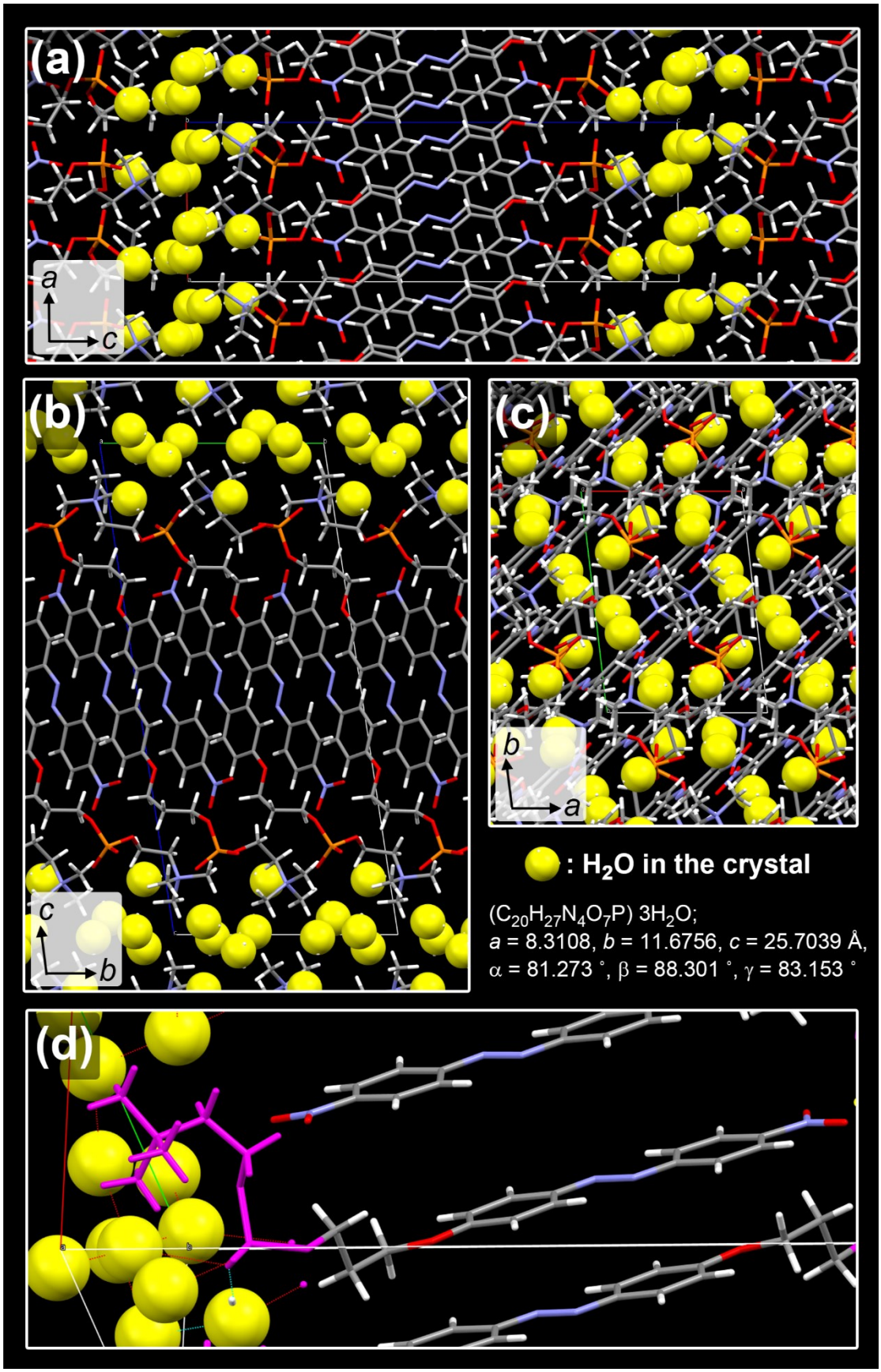


**Figure S2.** An X-ray single crystal structure of **N3**.

**3. Calculation of dipole moment of azobenzene derivatives by Spartan**

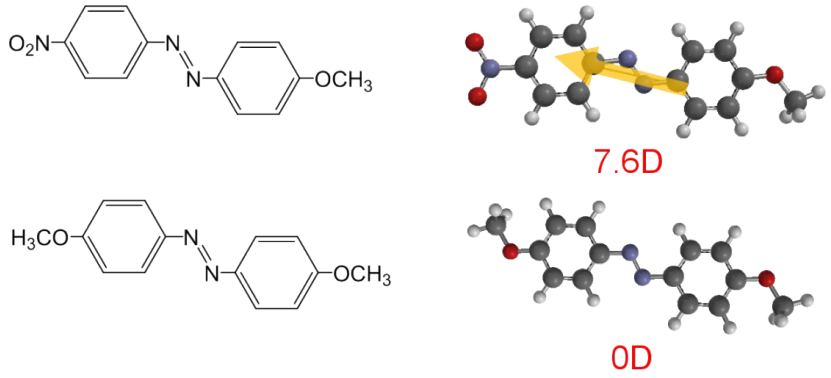


**Figure S3.** The dipole moment of **Az** compounds calculated by Spartan

**4. Consideration about sheet-like bilayer structure formation by van der Waals forces.**

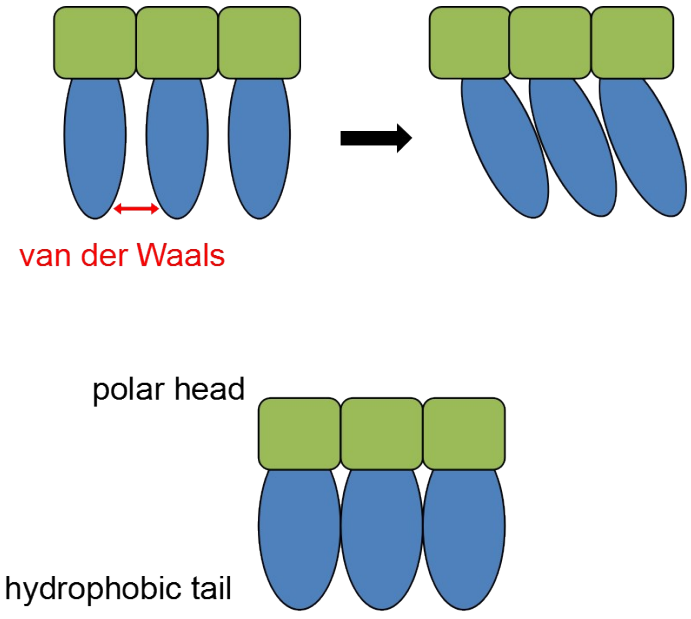


**Figure S4.** A schematic representation of the packing of lipid molecules with a polar head and a hydrophobic tail.

## 5. Effect of hydrophilic moiety on the formation of *H*-aggregates

As shown in Figure S5(a), the blue shift was not observed when the concentration of **NAz6TM** increased. It suggested that the **NAz6TM** molecules in water did not assembled into aggregation even at a higher concentration. As shown in Figure S5(b), the same situation was also found in the mixture of **NAz6TMA** and **MAz6TMA** in water.

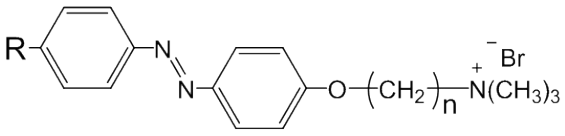


| | R | n |
|---|---|---|
| MAz6TMA | CH3O | 6 |
| NAz6TMA | NO2 | 6 |

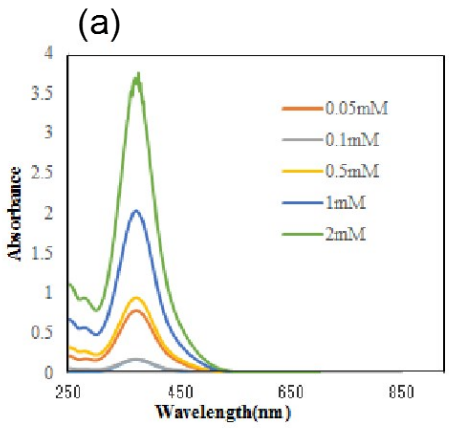


**Figure S5.** Absorption spectra of (a) **NAz6TMA**; (b) a mixture of **NAz6TMA** and **MAz6TMA** (***R*** = 50/50) in water

## 6. Changes in absorption spectra and surface tension by the change in the concentration of the mixture of N6/M6 in water (*R* = 50/50)

As shown in Figure S6(a), an absorption band at approximately 362 nm was observed at lower concentration in water (e.g. $c$ = 0.05 mM). The wavelength of the absorption band was shifted to shorter wavelength (329 nm) by increasing the concentration (e.g. $c$ = 1.0 mM). The blue shift of this band with increasing concentration was due to the formation of *H*-aggregates, and the driving force is furtherly enhanced by the stacking of the **Az** moieties. Figure S6(b) shows the changes in $A_{362}/A_{329}$ and the surface tension as a function of concentration of **N6/M6** mixtures in water. An abrupt change in $A_{362}/A_{329}$ as well as the surface tension was both observed at approximately 0.1 mM. These results indicate that self-assembly behavior of these molecules in *H*-aggregation occurs at concentrations higher than 0.1 mM of **N6/M6** mixture in water.

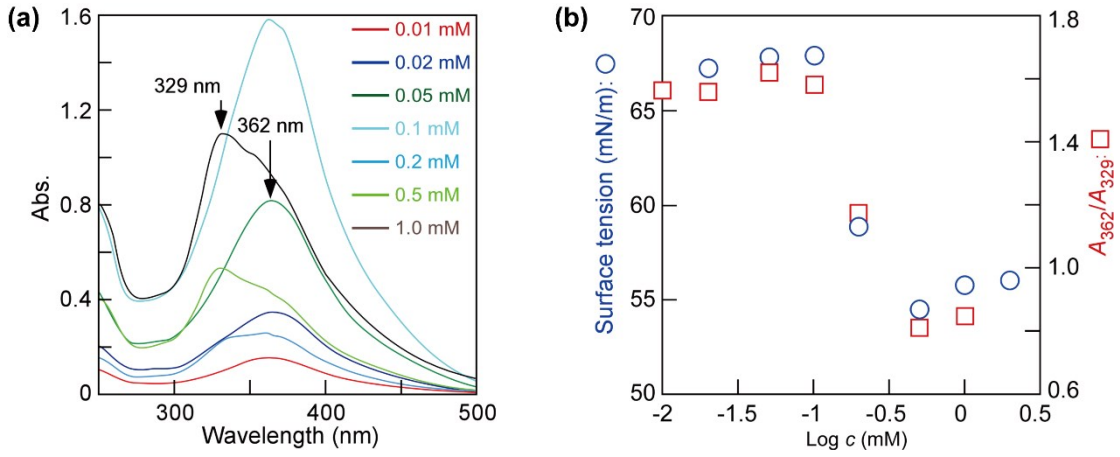


**Figure S6.** Changes in absorption spectra (a) and surface tension and $A_{372}/A_{350}$ as a function of concentration of the mixture of **N6** and **M6** (***R*** = 50/50) (b) in water.

## 7. $^1$HNMR characterization to form self-assembled vesicles in water

The solubility of **Az**-containing phospholipids is poor at room temperature, which resulted in the concentration of samples too low and signals too weak to be detected. Therefore, $^1$H NMR measurements were performed at 60 °C in $D_2O$ to investigate interactions between **N6** and **M6** (Figure S7). When measuring **M6** in $D_2O$ at 60 °C using $^1$H NMR, one of sharp peaks was obtained at 7.7 (δ/ppm), corresponding to the symmetrical aromatic hydrogens (-ArH-N=, 4H) (**M6**-a). Meanwhile, the peak at 7.8 (δ/ppm), was assigned to the aromatic hydrogens ($O_2N$-ArH-, 2H) (**N6**-a) of **N6**. However, a relatively broadened and shifted peak was observed at 7.51 (δ/ppm) for the **M6**-a and **N6**-a, when incubated **N6**/**M6** mixture in $D_2O$ at 60 °C. The reason for the chemical shifts and broaden peaks was that electrostatic interactions was introduced between the groups MeO- and $O_2N$-. Consequently, the change of hydrogen environment drove the occurrence of chemical shifts and broadened peaks.

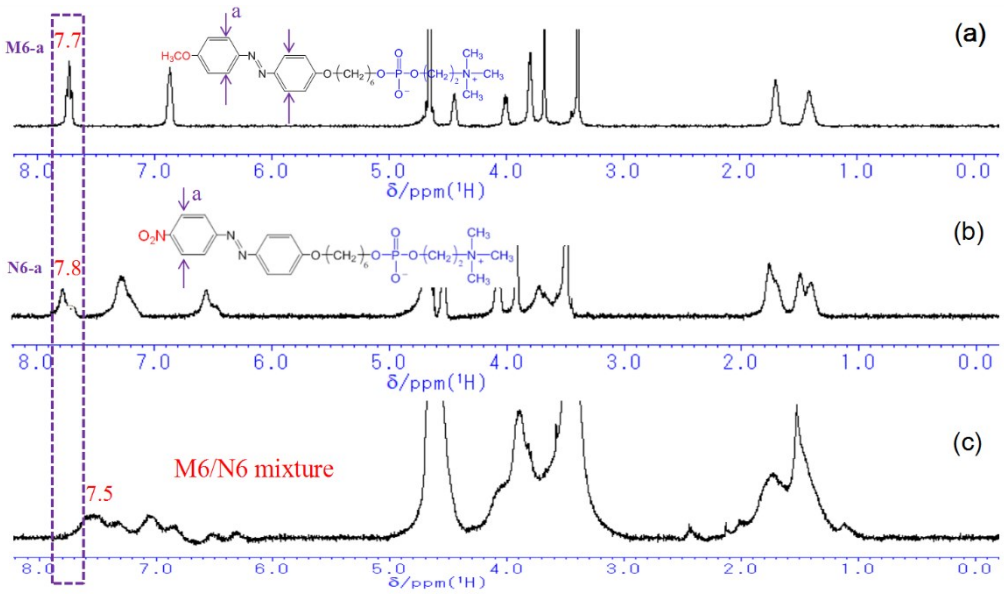


**Figure S7**. $^1$H NMR of **M6** (a), **N6** (b) and **M6**/**N6** mixture (***R*** = 50/50, *c* = 2 mM) (c) in $D_2O$ at 60 °C.

**8. A plausible self-assembled bi-layer structures by mixing M6 to N6**

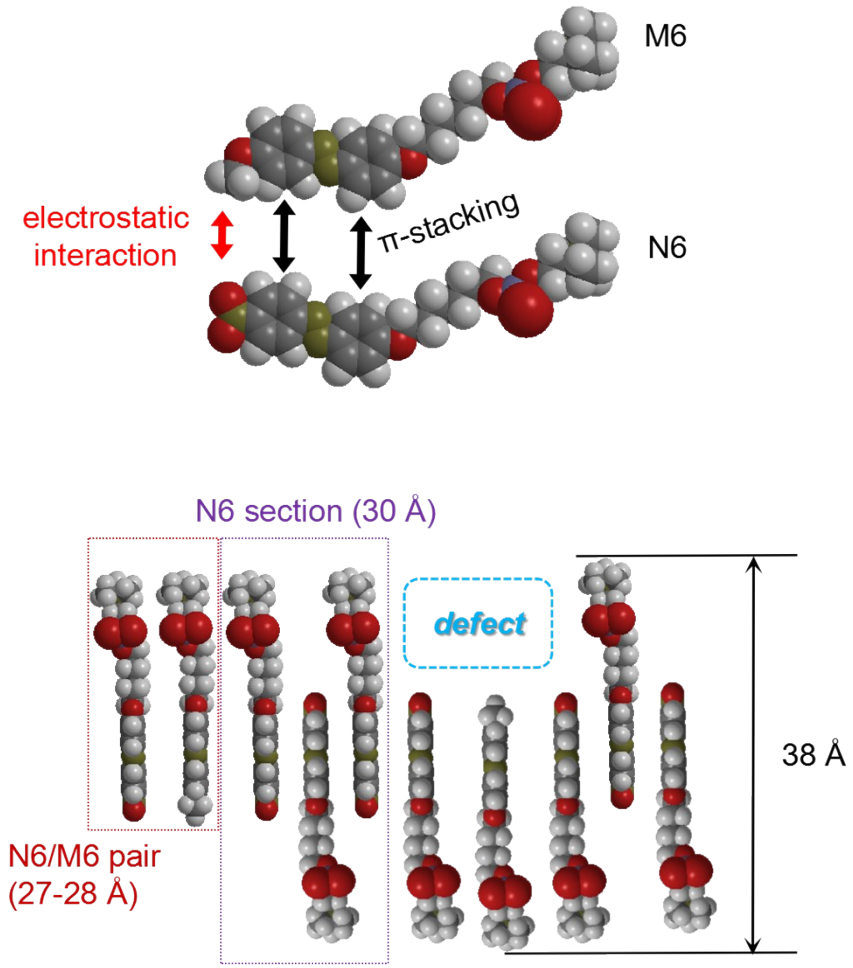


**Figure S8.** A plausible model for the molecular orientation of **N6** and **M6** (***R*** = 50/50) in the aggregation.

## 9. SAXS characterization of freeze dried N6/M6 mixtures in water with different mixing ratio

Figure S9 exhibits SAXS profiles of **N6**/**M6** mixtures prepared by freeze-drying from water dispersions. All the scattering profiles were taken at SPring-8 BL-03XU. Four peaks at 23, 27, 30, 38 Å were mainly observed, and the peak profiles were changed by the change in the **N6**/**M6** mixing ratio. By the comparison with the results shown in Figure 2, the scattering at 38 Å could be assigned as the bilayer thickness of the vesicles. On the other hand, peaks at 30 and 27 Å were due to layer thickness of **N6** and **M6** crystalline powders. As shown in Figure 2, there was neither phase separation nor recrystallization of **N6** and **M6**. In spite of careful treatment, freeze drying process might influenced the crystal formation. Further, an unassignable broad scattering at 23 Å were sometimes observed.

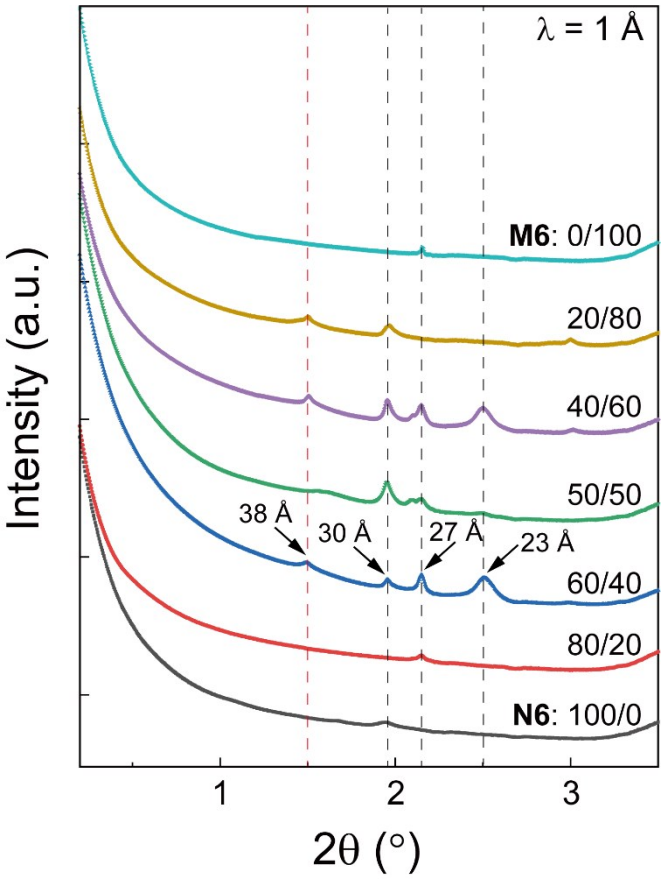


**Figure S9.** SAXS profiles of **N6**/**M6** mixtures prepared by freeze-drying from water dispersions. The total molar concentration of **N6** and **M6** in the dispersions was fixed to 2 mM.

**10. Changes in DLS profiles of N6/M6 vesicles (*R* = 50/50, *c* =2 mM) by irradiation with UV light**

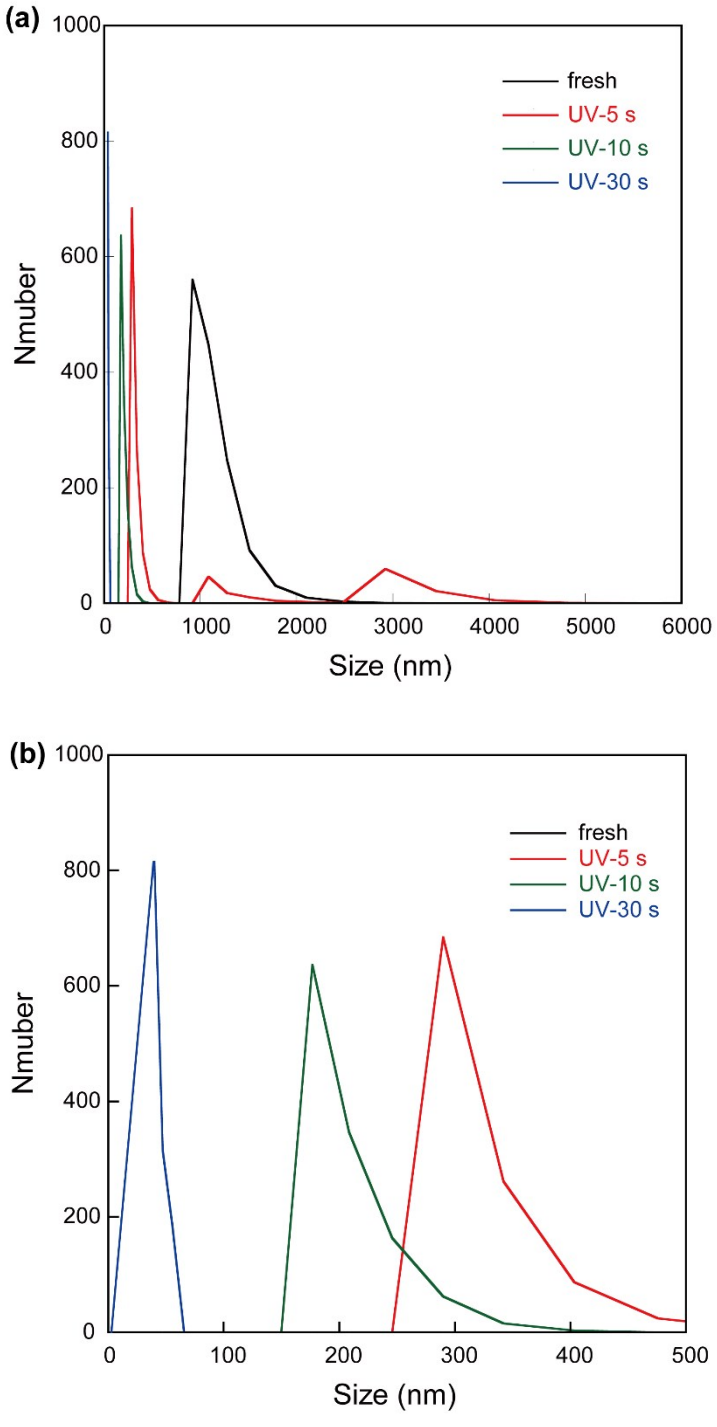


**Figure S10.** (a) Changes in DLS profiles of **N6**/**M6** vesicles (***R*** = 50/50, *c* =2 mM) by irradiation with UV light (365 nm,16 mW/cm$^2$); (b) the expanded image of (a).

**11. Changes in the absorption spectra of the vesicles as a function of irradiation time of UV light**

The **N6**/**M6** mixture (***R*** = 50/50, *c* = 0.5 mM) in water are vesicles with an average diameter of ca. 500 nm, which has been presented in Figure S11. Then, the changes in the absorption spectra of the vesicles as a function of irradiation time of UV light was detected. As shown in Figure S12, before UV irradiation, there was an absorption band at 340 nm, corresponding to the *H*-aggregation. The UV irradiation respectively caused the decrease and increase in absorbance at 340 nm and at 450 nm due to the photoisomerization of the **Az** groups in **N6** and **M6** from *trans*-form to *cis*-one, and the reverse situation was observed upon visible light irradiation less than 30 s.

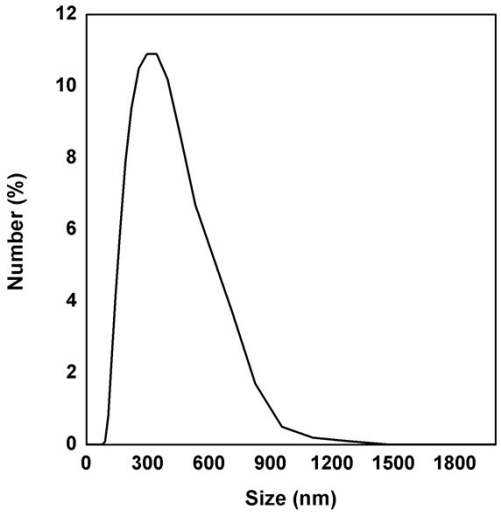


**Figure S11.** Average mean size of **N6**/**M6** vesicles (***R*** = 50/50, *c* = 0.5 mM) in water determined by DLS measurement.

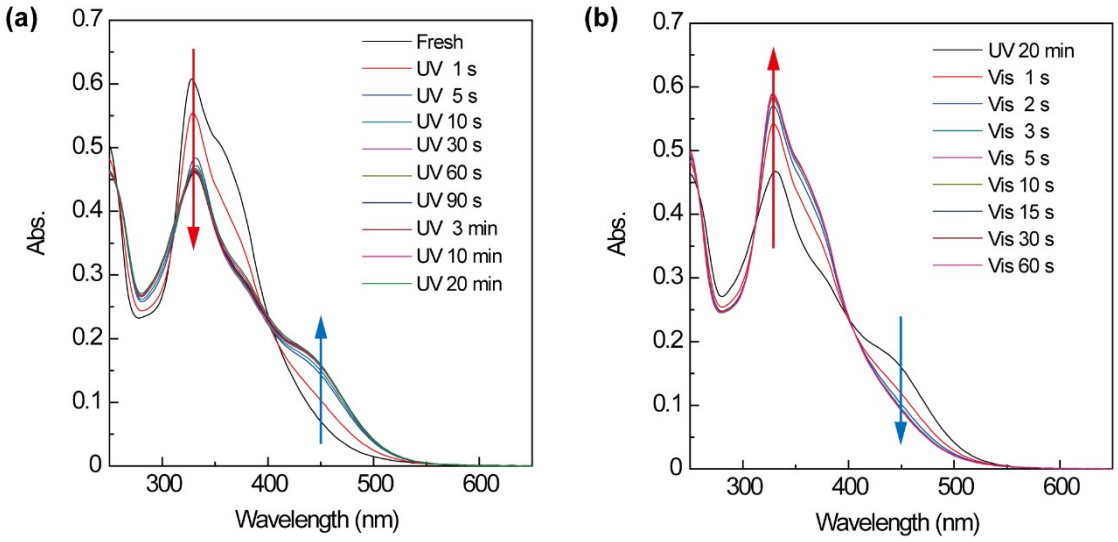


**Figure S12.** Changes in absorption spectra of the **N6/M6** mixture ($R$ = 50/50, $c$ =0.5 mM) in water by irradiation of UV light (365 nm, 1 mW/cm$^2$) and following visible light (436 nm,16 mW/cm$^2$).

**12. Changes in DLS profiles of N6/M6 vesicles (*R* = 50/50, *c* =2 mM) by visible light irradiation**

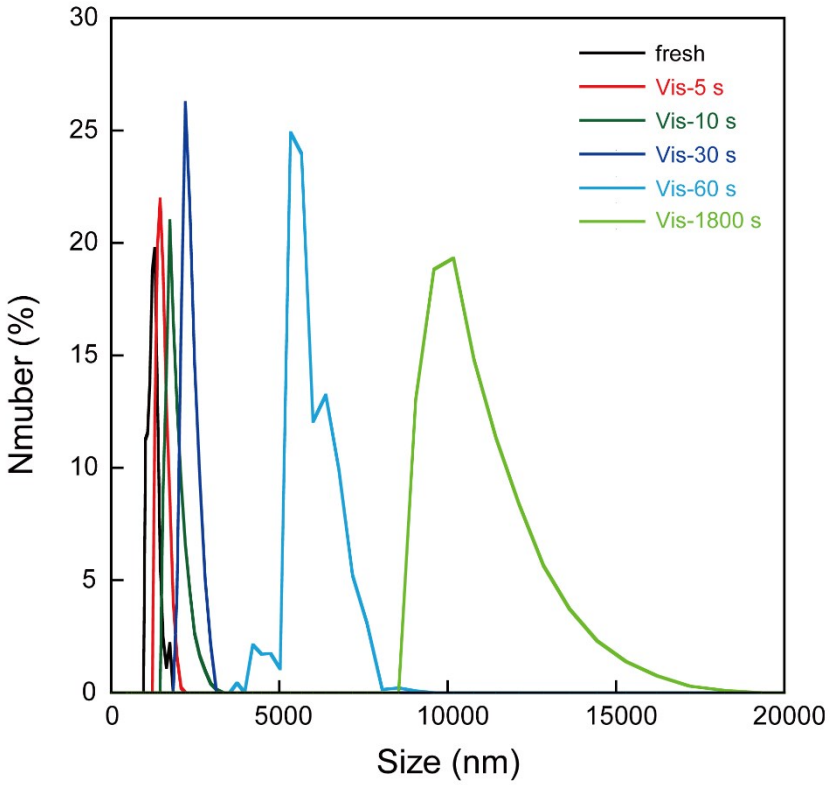


**Figure S13.** Changes in DLS profiles of **N6**/**M6** vesicles (***R*** = 50/50, *c* =2 mM) by visible light irradiation (436 nm, 16 mW/cm$^2$).

**13. Changes in absorption spectra of the M6/N6 vesicles (*R* = 50/50, *c* = 0.5 mM) in water by irradiation of visible light**

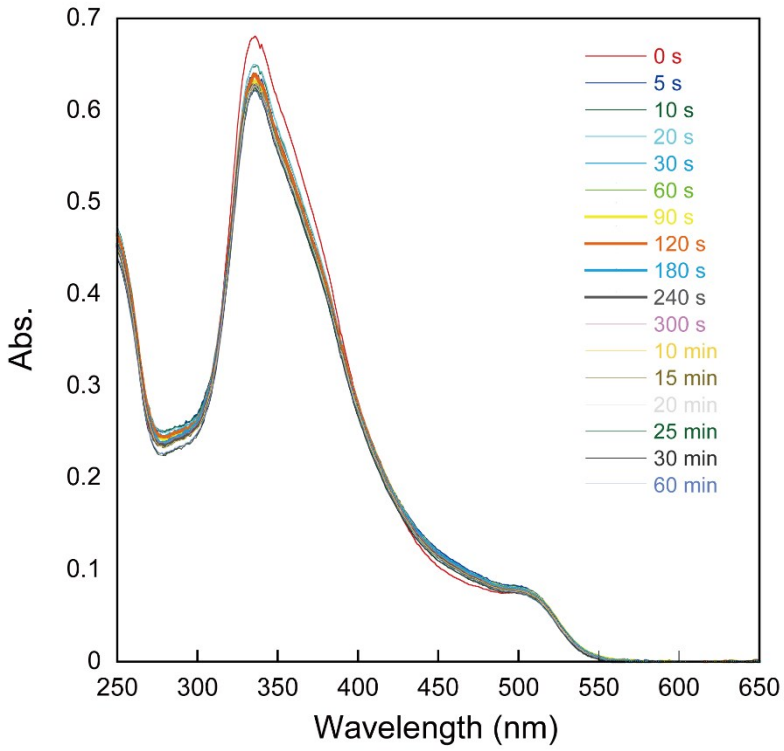


**Figure S14.** Changes in absorption spectra of the **M6**/**N6** vesicles (***R*** = 50/50, *c* = 0.5 mM) in water by irradiation of visible light (436 nm,16 mW/cm$^2$)